Characterization of the Temperature- and Pressure-Induced Inverse and Reentrant Transition of the Minimum Elastin-Like Polypeptide GVG(VPGVG) by DSC, PPC, CD, and FT-IR Spectroscopy

C. Nicolini,* R. Ravindra,* B. Ludolph,† and R. Winter*
*Department of Chemistry, University of Dortmund, Dortmund, Germany; and †Max-Planck Institute of Molecular Physiology, Dortmund, Germany

ABSTRACT We investigated the temperature- and pressure-dependent structure and phase behavior of a solvated oligopeptide, GVG(VPGVG), which serves as a minimalistic elastin-like model system, over a large region of the thermodynamic phase field, ranging from 2 to 120°C and from ambient pressure up to ~10 kbar, applying various spectroscopic (CD, FT-IR) and thermodynamic (DSC, PPC) measurements. We find that this octapeptide behaves as a two-state system which undergoes the well-known inverse-temperature folding transition occurring at $T \approx 36$°C, and, in addition, a slow trend reversal at higher temperatures, finally leading to a reentrant unfolding close to the boiling point of water. Furthermore, the pressure-dependence of the folding/unfolding transition was studied to yield a more complete picture of the p,T-stability diagram of the system. A molecular-level picture of these processes, in particular on the role of water for the folding and unfolding events of the peptide, presented with the help of molecular-dynamics simulations, is presented in a companion article in this issue.

INTRODUCTION

Elastin, a principle protein component in vertebra's connective tissues, and its precursor, tropoelastin, feature very unusual viscoelastic properties (Urry, 1993, 1997; Urry et al., 2002). Most interesting is the peculiarity that folding of these proteins is achieved by increasing the temperature beyond typically 40°C. In fact, it is remarkable that with the proper amino acid composition, proteins are able to give rise to more organized structures when heating to raise the temperature. For the elastins, these are temperatures at which normal proteins (such as lysozyme, SNase, or RNase A) undergo unfolding and denaturation. The term *inverse temperature transition* (ITT) was coined for this apparently paradoxical change from a disordered (extended) to an ordered (folded) conformation upon heating. On first sight, this increase in order on raising the temperature would seem to contradict the second law of thermodynamics that the order of a system decreases on increasing the temperature. The apparent contradiction resolves, of course, once the total system, i.e., the protein with its surrounding hydration sphere, is considered. This also immediately elucidates that the structural and dynamic properties of water markedly influence the protein's behavior, a point which is in the focus of a companion theoretical article (Rousseau et al., 2004). Interestingly, it has been pointed out that protein-based polymers comprised of elastin's particular properties are capable of performing many of the energy conversions that sustain life and may be used for designing biomolecular machines (Urry, 1997; Urry et al., 2002).

The origin of elastin's properties is controversially discussed, recalling concepts such as classical rubber elasticity, various librational entropy mechanisms, hydrophobic collapse, multiphase models, and iceberg/clathrate formation (Urry, 1993, 1997; Urry et al., 2002; Rousseau at al., 2004; Debelle and Tamburro, 1999; Li et al., 2001a,b; Blokzijl and Engberts, 1993; Tarek and Tobias, 1999, 2002a,b). Even tropoelastin is a complex protein and its structure still defeats elucidation on a molecular level. Fortunately, there is consensus that the pentameric repeat unit VPGVG (amino acids valine, *V*; proline, *P*; and glycine, *G*) is crucial to elastin's functionality making it the basic sequence of various synthetic mimetica (Reiersen et al., 1998). Most interestingly, it was recently demonstrated that polypentapeptides of the kind $GVG(VPGVG)_n$ display the ITT even in the limit $n = 1$. This opens up the possibility for us to scrutinize the ITT based on well-defined small model biopolymers. We therefore have launched a joint experimental/simulation study of the octamer GVG(VPGVG) (*molecular mass* ≈ 640 Da); see the companion article (Rousseau et al., 2004), and our preliminary short communication (E. Schreiner, C. Nicolini, B. Ludolph, R. Ravindra, N. Otte, A. Kohlmeyer, R. Rousseau, R. Winter, and D. Marx, unpublished material). This minimalistic elastin model was chosen to allow for extensive molecular-dynamics (MD) simulations with a thorough conformational mapping followed by an in-depth

Submitted September 26, 2003, and accepted for publication November 10, 2003.

Address reprint requests to R. Winter, Dept. of Chemistry, Physical Chemistry I, University of Dortmund, Otto-Hahn Str. 6, D-44227 Dortmund, Germany. Tel.: 49-231-755-3900; E-mail: winter@pci.chemie.uni-dortmund.de.

Abbreviations used: Boc, tButyloxycarbonyl; DHB, 2,5-dihydroxybenzoic acid; DIPEA, diisopropylethylamine; DMF, dimethylformamide; DSC, differential scanning calorimetry; ESI, electron spray ionization; FAB, fast atom bombardment; Fmoc, fluorenylmethoxycarbonyl; HBTU, 2-(1 H-benzotriazol-1-yl)-1,1,3,3-tetramethyluroniumhexafluorophosphate; HOBt, *n*-hydroxybenzotriazole; HPLC, high performance liquid chromatography; HRMS, high resolution mass spectroscopy; LCMS, liquid chromatography mass spectrometry; MALDI, matrix-assisted laser desorption/ionization; 3-NBA, 3-nitrobenzyl alcohol; TFA, trifluoroacetic acid.

0006-3495/04/03/1385/08 $2.00

statistical mechanical analysis. To yield experimental information about changes in secondary structure, circular dichroism (CD) and Fourier-transform infrared (FT-IR) spectroscopic measurements were carried out, supplemented by new thermodynamic information on the heat capacity and thermal expansion coefficient. The absence of any reactive side chain means that the protein is stable over long periods of time even at rather high temperatures, thus allowing the exploration of its structural properties even at temperatures as high as the boiling point of water and beyond, which was a further goal in our studies. To yield a more complete thermodynamic description of the system, we not only investigated the temperature-dependence, but also the pressure-dependence of the structural properties of the system. In recent years the study of the effects of pressure on biological systems has in fact drastically expanded (Heremans and Smeller, 1998; Winter, 2002; Winter and Jonas, 1999; Balny et al., 2002; Klink et al., 2003). In particular, pressure has been used for studying pressure-induced un/refolding of proteins and for understanding protein stability and its folding pathways. Furthermore, pressure studies have been applied to elucidate survival strategies of deep sea organisms, because studies of proteins from extremophile bacteria bear biotechnological potential, mainly in the fields of food science and pharmaceutical industry.

MATERIALS AND METHODS

Synthesis of the peptide GVG(VPGVG)

Solid-phase peptide synthesis with an Fmoc-protecting group strategy and chlorotrityl (2ClTrt) linker was employed to synthesize the peptide sequence GVG(VPGVG). With 313 mg of commercially available 2ClTrt polystyrene resin preloaded with glycine (loading 0.8 mmol/g, 0.25 mmol) repetitive coupling and deprotection steps with the corresponding Fmoc amino acid (4 equivalents (eq.)), HBTU (3.6 eq.), HOBt (4 eq.), and DIPEA (8 eq.) in DMF and piperidine/DMF 4:1, respectively, were carried out leading to the resin-bound target peptide. Last glycine amino acid was protected with a Boc group instead of Fmoc. The peptide was cleaved from resin with acetic acid/trifluorethanol/dichlormethane 1:1:3 and treated with 50% TFA to remove the Boc group. Purification was achieved by preparative HPLC (retention time of product was 20.5 min; with C18PPN column, flow rate was 15 mL/min; solvent A was H_2O, solvent B was acetonitrile; the gradient at 0 min, for A, was 95%, for B, was 5%; at 13 min, A was 95%, B was 5%; and at 30 min, A was 65%, B was 35%) to give 54 mg (0.084 mmol, 34%) of pure peptide. For $[\alpha]_D^{20} = -22.3°$ ($c = 0.13$ g/L in MeOH), ^{1}H-NMR (400 MHz, MeOD): δ/ppm = 4.46–3.60 (*m*, 12H, 4× α-CH_2 Gly, 4× α-CH), 2.25–1.94 (*m*, 7H, 2× CH_2 Pro, 3× CH Val), and 0.99–0.91 (*m*, 18H, 6× CH_3 Val). LCMS (ESI): HPLC retention time is 10.4 min; with C18PPN column, flow rate was 1 mL/min; solvent A was H_2O with 0.1% HCOOH, solvent B was acetonitrile with 0.1% HCOOH; the gradient at 0 min, for A, was 90%, for B, was 10%; and at 20 min, A was 70%, B was 30%. ESI: calculated for [M+H] 641.35, [2M+H] 1281.70, and [M-H] 639.35; found (*m*/+z) 641.3, 1281.4; and (*m*/−z) 639.5. MALDI (DHB): calculated for [M+H] 641.4, [M+Na] 663.3; found 641.8, 663.8. HRMS (FAB, 3-NBA): calculated for [M+Na] 663.3442; found 663.3417.

CD spectroscopy

The GVG(VPGVG) peptide was dissolved at concentrations of 1 and 0.5 mg/mL in 10 mM phosphate buffer at pH 7. The concentrations were determined spectrophotometrically using the absorption coefficient at 225 nm. CD spectra were recorded between 2 and 95°C in a cylindrical thermocell (1-cm pathlength) from 190 to 260 nm on a JASCO J-715 (Easton, MD) spectropolarimeter under constant nitrogen flush. Owing to the design of the sample cell, measurements at higher temperatures (>100°C) could not be performed with this method. An external water thermostat was used for temperature-dependent measurements to control the temperature within 0.1°C. Temperature-dependent CD scans were carried out by first cooling the sample to 2°C and then stepwise increasing the temperature from 2 to 95°C, and allowing the samples to equilibrate at each temperature for 15 min. CD data are expressed as the mean residual ellipticity (MRE) [θ] in degrees cm^2 $dmol^{-1}$. The secondary structure content of the peptide in solution was determined using convex constraint analysis (Perczel et al., 1991, 1992) with two conformational states (β-turns/strands and unordered conformations). Ellipticities were found, within the limit of experimental error, to be independent of the peptide concentration of a few mg/mL, indicating that the temperature-induced conformational changes are due to intramolecular interactions rather than intermolecular associations.

FT-IR spectroscopy

The peptide was dissolved at a concentration of 5% (w/w) in 10 mM TRIS buffer (Sigma, St. Louis, MO) with 99.9% D_2O (Sigma) at pD 7 for the high-pressure experiments. For the temperature-dependent experiments, we used a 10 mM phosphate buffer. The pD of the solution was adjusted to 7.0 using DCl. The FT-IR spectra were recorded with a Nicolet MAGNA 550 spectrometer (Thermo Electron GmbH, Dreieich, Germany) equipped with a liquid-nitrogen-cooled MCT (HgCdTe) detector. For the pressure-dependent measurements, the infrared light was focused by a spectral-bench into the pinhole of a diamond anvil cell with type IIa diamonds (Panick et al., 1998; Reis et al., 1996; Siminovitch et al., 1987; Herberhold et al., 2003). Each spectrum was obtained by co-adding 512 scans at a spectral resolution of 2 cm^{-1} and was apodized with a Happ-Genzel function. The sample chamber was purged with dry and carbon dioxide free air. Powered α-quartz was placed in the hole of the steel gasket of the diamond anvil cell and changes in pressure were quantified by the shift of the phonon band of quartz appearing at 695 cm^{-1} (Siminovitch et al., 1987). The temperature-dependent measurements were carried out using a cell with CaF_2 windows separated by 50-μm Teflon spacers. An external water thermostat was used for the pressure- and temperature-dependent measurements to control the temperature within 0.1°C. The equilibration time before recording spectra at each temperature and pressure was 15 min. Fourier self-deconvolution of the IR spectra was performed with a resolution enhancement factor of 1.8 and a bandwidth of 15 cm^{-1}. The fractional intensities of the secondary structure elements were calculated from a bandfitting procedure using Gaussian-Lorentzian lineshape functions (Panick et al., 1998; Herberhold et al., 2003).

Differential scanning and pressure perturbation calorimetry

A complementary differential scanning calorimetry (DSC) set of thermodynamic data could be obtained from pressure perturbation calorimetry (PPC)—a rather novel method that allows us to measure heat effects induced by small periodic changes of gas pressure above a protein solution. The physical principle is the same as in a heat-induced thermal expansion, although the measurable is ΔQ—the heat released upon a pressure change of Δp at temperature T. Knowing the thermal expansion coefficient of the solvent, α_0, the mass, m_s, and partial specific volume, $\overline{V}_s$, of the solute, through a series of reference measurements, one can calculate the apparent thermal expansion coefficient of the dissolved particle (Lin et al., 2002; Ravindra and Winter, 2003a,b), as

$$\alpha = \alpha_0 - \frac{\Delta Q}{T\,\Delta p\, m_s\, \overline{V}_s}. \quad (1)$$

PPC yields α versus T plots, which largely reflect the kosmotropic (mostly hydrophobic) or chaotropic (polar and charged) character of the amino acid side-chain residues interacting with the surrounding solvent. Dramatic changes in α-T curves observed upon thermal denaturation of proteins arise from different water-structuring properties of amino acids being exposed to the bulk solvent upon unfolding from those interacting with the solvent in the native state, and from the corresponding changes of the surface-accessible surface area (SASA) which changes the ratio of hydrophobic versus hydrophilic residues upon unfolding. A more comprehensive description of the theory and methodology of PPC was given elsewhere (Lin et al., 2002; Ravindra and Winter, 2003b). The heat capacities, C_p, and thermal expansion coefficients, α, were obtained up to 120°C from DSC and PPC measurements, respectively. The measurements were carried out on a VP calorimeter from MicroCal (Central Milton Keynes, UK) equipped with a PPC accessory. For all DSC experiments, a gas pressure of ~4 bar was applied to prevent evaporation of the solvent at the highest temperatures measured. The instrument was in the high-gain mode and a rate of 40 K/h was used. Sample concentration was 0.5–1.0 wt % peptide in 10 mM phosphate buffer.

RESULTS AND DISCUSSION

Analysis of the temperature-dependent CD measurements

The CD spectra of the GVG(VPGVG) peptide (0.5 mg/mL in 10 mM phosphate buffer, pH 7) taken at various temperatures are shown in Fig. 1. At 2°C, the spectrum consists of a large negative band at 197 nm and a small one at 220 nm. The minimum MRE is $-7000°$ cm^2 dmol^{-1} and shifts slightly from 197 to 200 nm upon increasing the temperature. Typically, random or disordered polypeptide structures exhibit a CD minimum at ~195 nm, with an intensity of $\sim -40{,}000°$ cm^2 dmol^{-1}, however (Provencher and Glöckner, 1981). In our case, the amplitude of the negative band is lower than the generally observed value for large random polypeptide structures. Such a difference is not unexpected in view of the short peptide (8-mer) under investigation. The larger MRE value might also be due to the presence of some remaining order, however. Upon heating, the two minima shift such that an isodichroic point is observed at ~212 nm which indicates the presence of two main conformational states. As shown in the inset of Fig. 1, no dichroic zone but rather a true dichroic point can be inferred from the data within the accuracy of the experiment. A near-isodichroic point for different elastin peptides was also detected by Urry et al. (1985) and Reiersen et al. (1998) at ~218–220 nm. The temperature-dependence of some characteristic spectral features of the CD spectra of the sample is shown in Fig. 2. When the temperature increases, the amplitude of the band at 197 nm decreases by ~5000 MRE units moving to larger residual ellipticity values, whereas the shallow minimum at 220 nm increases concomitantly. The developing positive peak in the 206–212 nm spectral region is characteristic of type II β-turns (Provencher and Glöckner, 1981). The reversibility of the conformational transition was tested by heating the sample to 95°C and subsequent cooling to 20°C in 12 h. The transition was found to be largely reversible (>90%) in this time range and does not seem to depend significantly on the peptide concentration.

For the analysis of the secondary structure elements, the Provencher and Glöckner method (Provencher and Glöckner, 1981), as suggested by Debelle and co-workers (Debelle and Alix, 1999; Debelle et al., 1998), was applied first. This method is based on a linear combination of the CD spectra of proteins, whose secondary structures are known from x-ray crystallography. The results obtained are unsatisfactory, however, because the reference proteins are much larger than our only 8-amino-acids-long peptide, which is unable to develop well-defined secondary structures. Hence, we used

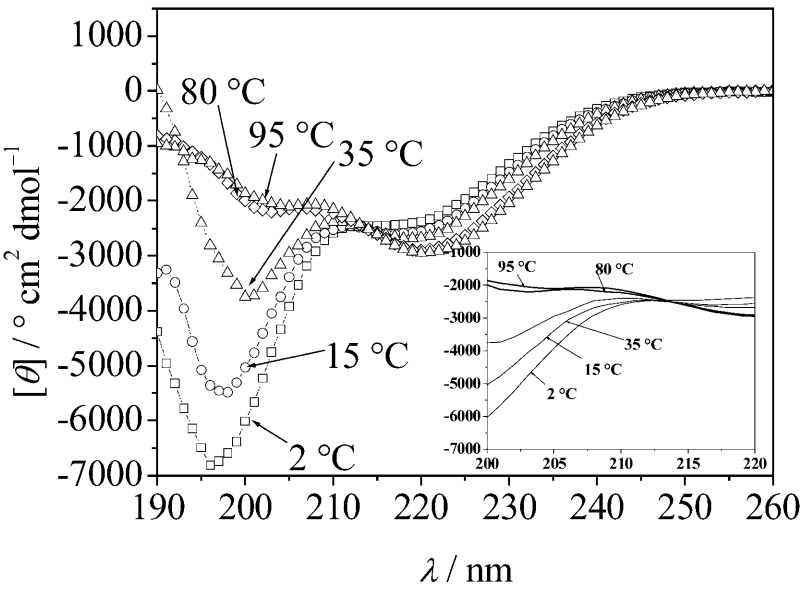

FIGURE 1 CD spectra of the peptide GVG(VPGVG) at selected temperatures in the temperature range from 2 to 95°C, 0.5 mg/mL peptide in 10 mM phosphate buffer, pH 7.0. (*Inset*) Blowup of the CD spectra around the dichroic point (curves present fits to the data points).

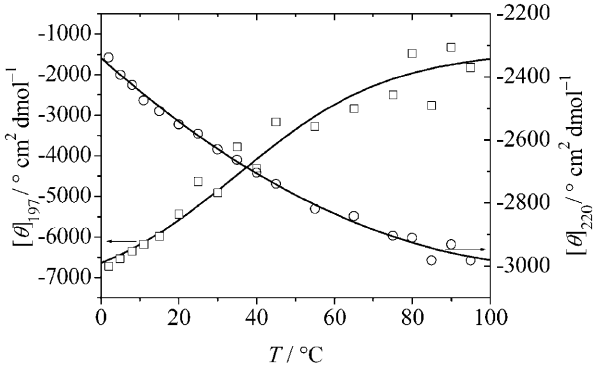

FIGURE 2 Temperature-dependence of the mean residual ellipticity of the peptide GVG(VPGVG), 0.5 mg/mL in 10 mM phosphate buffer, pH 7.0, at 197 nm (□) and 220 nm (○), respectively. The fit function to the data is a sigmoidal function.

the convex constraint algorithm for deconvoluting the CD spectra in its pure components (Perczel et al., 1991, 1992). We chose $P = 2$ as the number of pure components for the deconvolution as suggested by the appearance of an isodichroic point. The quality of the fit was checked through the root-mean square value, which for $P = 2$ is <10. The use of a higher number of components did not improve the fits and resulted in unreasonable and unsystematic conformational weights. The results are in agreement with the existence of two main conformational states: one state, dominating at low temperatures, consists of disordered structures and γ-loops; the second, prevailing at higher temperatures, consists of β-turns/strands. As shown in Fig. 3, the unordered structures decrease by 37 ± 3% over the whole temperature range covered, whereas the β-turn structures increase concomitantly. Although the analysis of the molar ellipticities at 212 and 220 nm yields a formal transition temperature of ~36°C, the ITT is very sluggish and broad for this octapeptide.

Temperature-dependent FT-IR spectroscopic measurements

To confirm the effect of temperature on the secondary structure of GVG(VPGVG) by an additional method, we measured the temperature-induced changes in the amide I′ region (1575 to 1700 cm^{-1}) of the infrared spectrum (Panick et al., 1998) in the temperature range between 2°C and 95°C using D_2O as solvent at pD 7.0 (Fig. 4). The secondary structure elements are assigned to IR bands as summarized in Table 1 (Byler and Susi, 1986; Pestrelski et al., 1991; Dzwolak et al., 2002). The band at ~1675 cm^{-1} can be assigned to type II β-turns, the bands at 1660 and 1654 cm^{-1} are associated with turn-and-loop structures, and the band at 1641 cm^{-1} is assigned to disordered structures. The two other bands that appear at 1617 and 1595 cm^{-1} are probably due to the IR absorption of the terminal COO^- group in two different conformational states. The band at 1595 cm^{-1} is typical for the COO^- terminal group of proteins (Tamm and Tatulian, 1997). As the origin of the band at 1617 cm^{-1} was unclear, we measured the IR spectrum of a mixture of the pure amino acids G, V, and P in the same concentration ratio as contained in the protein and under the same experimental conditions. A broad band observed at ~1617 cm^{-1} (data not shown) indicates in fact that carboxyl groups may absorb in this wavenumber region. Hence, we may assume that the two bands correspond to two different conformations and/or ionized states of the same carboxyl group. This is supported by the finding that the two bands exhibit an isosbestic point, if the spectra are corrected for their temperature dependence. Interestingly, this finding might also be related to a stretching-induced pK_a shift of the carboxyl groups as observed for elastin-like model polymers (Urry, 1997). The increase in pK_a on stretching of the hydrophobically folded protein means that the free energy of the carboxylate increases. The reason is thought to be the structure of water of hydrophobic hydration being unsuited for charged groups (Urry, 1997).

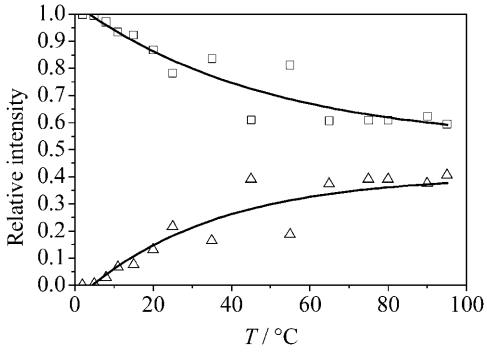

FIGURE 3 Temperature-dependence of the secondary structure elements of the peptide GVG(VPGVG), 0.5 mg/mL in 10 mM phosphate buffer, pH 7.0, as obtained from the convex constraint algorithm (□, disordered structures and γ-turns; △, β-loops/strands).

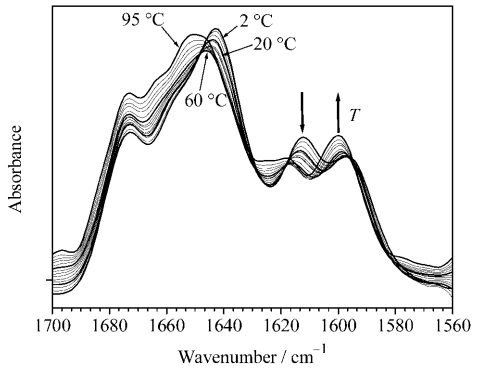

FIGURE 4 Deconvoluted FT-IR absorption spectra of the peptide GVG(VPGVG), 5% (w/w) in 10 mM phosphate buffer, pD 7.0, as a function of temperature at ambient pressure.

TABLE 1 Wavenumber of secondary structure elements in the amide I′ infrared region

Secondary structure element	Wavenumber/cm^{-1}
Extended β-chains	1615–1628
β-sheets	1620–1640
Disordered structures (random coil)	1640–1650
α-helices or loops/turns	1650–1658
Turns (β- and γ-turns)	1660–1690

See Byler and Susi (1986), Pestrelski et al. (1991), and Dzwolak et al. (2002).

The deconvoluted IR spectrum of GVG(VPGVG) at 2°C is characterized by a maximum at 1641 cm^{-1}, which is due to a high content of disordered secondary structures. The intensity of this band decreases with increasing temperature and shifts to larger wavenumbers, and a broad band appears at ~1650 cm^{-1}, which is characteristic for loop/turn structures (no α-helices can be formed for this small peptide). The evolution of the secondary structures of GVG(VPGVG) as a function of temperature, as obtained from fitting the spectra using six subcomponents according to the data given in Table 1, is shown in Fig. 5. With increasing temperature up to ~55°C, a significant decrease (~25%) of disordered structures and a concomitant increase in loop/turn structures is observed. These observations are thus in good agreement with the results obtained from the CD measurements. The trend of peptide folding upon heating clearly comes to a hold in the range of 60 to 80°C. Interestingly, at $T > 80$°C, a reversal of this behavior is observed: the weight of disordered conformations increases again at the expense of the loop/turn structures. A similar reversal is obtained from the intensities of bands at 1617 and 1595 cm^{-1}, which are assigned to different conformations of the terminal carboxyl group. In other words, there is evidence that the ITT is succeeded by a further unfolding transition, which takes place at temperatures approaching the boiling point of water.

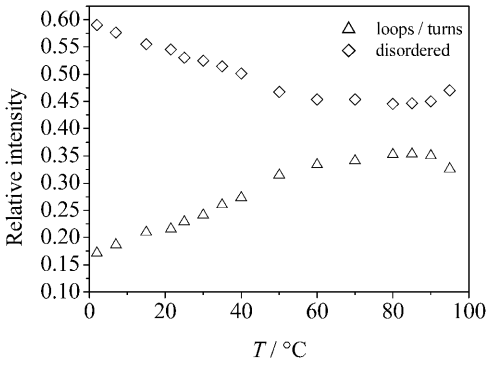

FIGURE 5 Temperature-dependence of the relative intensities of secondary structure elements (◇, random; △, loops) of GVG(VPGVG) as obtained from the FT-IR data.

Thermodynamic analysis

To determine the standard Gibbs free-energy change, ΔG^{o}, of the conformational transition as well as the corresponding enthalpy and entropy changes, the temperature-dependent CD data (at 197 nm) and FT-IR data (Figs. 3 and 5, respectively) were fitted to a two-state model. The van't Hoff plot (plot of ln$K$ versus $1/T$, K being the equilibrium constant) as obtained from the CD data is shown in Fig. 6. It was constructed from $K = ([\theta]^{obs} - [\theta]^{U})/([\theta]^{F} - [\theta]^{obs})$, where $[\theta]^{obs}$ are the CD data for the experimentally observed ellipticity, and $[\theta]^{F}$, $[\theta]^{U}$ the values for the previously fitted endpoints of the transition (high-temperature folded form, $[\theta]^{F}$, and low-temperature unfolded form, $[\theta]^{U}$. The data for ΔG^{o}, the enthalpy changes ΔH^{o}, and entropy changes ΔS^{o} are shown in Table 2 for selected temperatures. The corresponding data as obtained from the IR data are of similar magnitude (Table 2). We obtain an enthalpy change of 34 kJ mol^{-1} and an entropy change of 0.11 kJ mol^{-1} K^{-1} at room temperature, i.e., both values are positive. This supports the model of an entropy-driven, temperature-induced folding transition. The peptide exhibits an increase of more ordered, loop/turn-like structures at higher temperature, thus supporting the notion that the folding of this sequence might be a consequence of hydrophobic interactions that are driven by positive entropies of (partial) dehydration. Other scenarios that can be traced back to qualitative changes in the hydrogen-bond dynamics at the peptide/water interface might also play a significant role for this small polypeptide, and are discussed below.

Pressure-dependent FT-IR spectroscopic measurements

To study the effect of pressure on the secondary structures of GVG(VPGVG), we also measured the pressure-induced

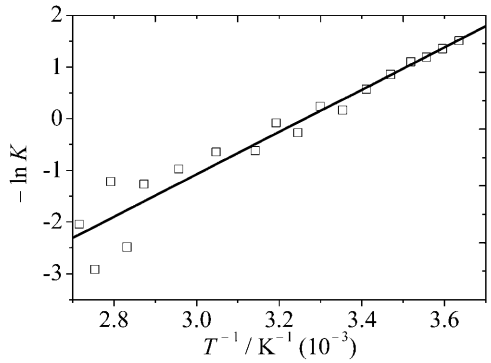

FIGURE 6 Van't Hoff plot as constructed from the CD data at 197 nm, which were fitted to the two-state model introduced in the text. By using the fitted endpoints of the transition, a linear van't Hoff plot is obtained, which allowed the calculation of the enthalpy change ΔH^{o}, entropy change ΔS^{o}, and transition temperature T_m of the conformational transition from the slope, ordinate, and $\Delta H^{o}/\Delta S^{o}$ values, respectively. The linear correlation coefficient is $r = 0.96$.

TABLE 2 Thermodynamic values of the temperature-induced conformational transition of the peptide GVG(VPGVG) as obtained from the CD and IR-spectroscopy data

T/°C	ΔH^0/kJ mol^{-1}	ΔG^0/kJ mol^{-1}	ΔS^0/kJ mol^{-1} K^{-1}
CD			
25	34 ± 16	0.61 ± 0.3	0.11 ± 0.05
33	34 ± 17	−0.21 ± 0.1	0.11 ± 0.05
75	34 ± 19	−7.2 ± 4.0	0.12 ± 0.07
IR			
25	47 ± 9	1.3 ± 0.2	0.15 ± 0.03
35	47 ± 9	−0.25 ± 0.05	0.15 ± 0.03
70	47 ± 10	−6.6 ± 1.4	0.16 ± 0.04

changes in the amide I′ region of the IR spectrum at 6, 25, 40, and 60°C in the pressure range from ambient pressure up to 10 kbar. The pressure-dependence of the deconvoluted FT-IR spectra of GVG(VPGVG) at pD 7.0 are shown in Fig. 7. With increasing pressure, the amide I′ band maximum shifts to smaller wavenumbers. The pressure-induced changes in the fractional intensities of the different amide I′ subbands are presented for the measurement at 6°C in Fig. 8. Within the experimental error (~6%), the fractional intensities of type II β-turn-and-loop structures decrease, whereas the population of disordered (nonperiodic) structures increases with increasing pressure. The secondary structural changes observed amount to ~30% over the whole pressure range up to 9 kbar. An analysis of the concentration profile as a function of pressure yields a volume change for the pressure-induced shift of the ordered-to-disordered state equilibrium of $\Delta V \approx -18 \pm 8$ mL/mol^{-1} (at 6°C). For the other temperatures, the changes in the fractional intensities take a similar profile. The pressure-induced structural changes observed were found to be fully reversible. Hence, pressure and temperature increase have contrary effects on the secondary structure of this elastin fragment for the pressure and temperature range covered in these experiments.

Differential and pressure perturbation calorimetric measurements

Further confirmation of the reentrant unfolding behavior at high temperature comes from very accurate thermodynamic measurements of both the apparent heat capacity, C_p, and the apparent thermal expansion coefficient, α, of the peptide as obtained by DSC and PPC measurements (see Figs. 9 and 10). The expansion coefficient largely reflects the kosmotropic or chaotropic character of the amino acid side-chain residues interacting with the surrounding water, and significant changes in α-T curves are observed upon thermal unfolding and denaturation of proteins, owing to changes in the SASA and the ratio of hydrophobic versus hydrophilic amino acid residues. At low temperatures, α is large, which would be consistent with a significantly hydrated extended or disordered structure (Lin et al., 2002). Thermal activation leads to a release of this condensed water from the peptide surface. Once the water is released, it no longer contributes to the partial volume of the peptide and hence to α. The decrease of α with increasing temperature is followed by a plateau region of low α-values from ~30–40°C to 80–90°C, where α increases again. Thus, the smallest α is found

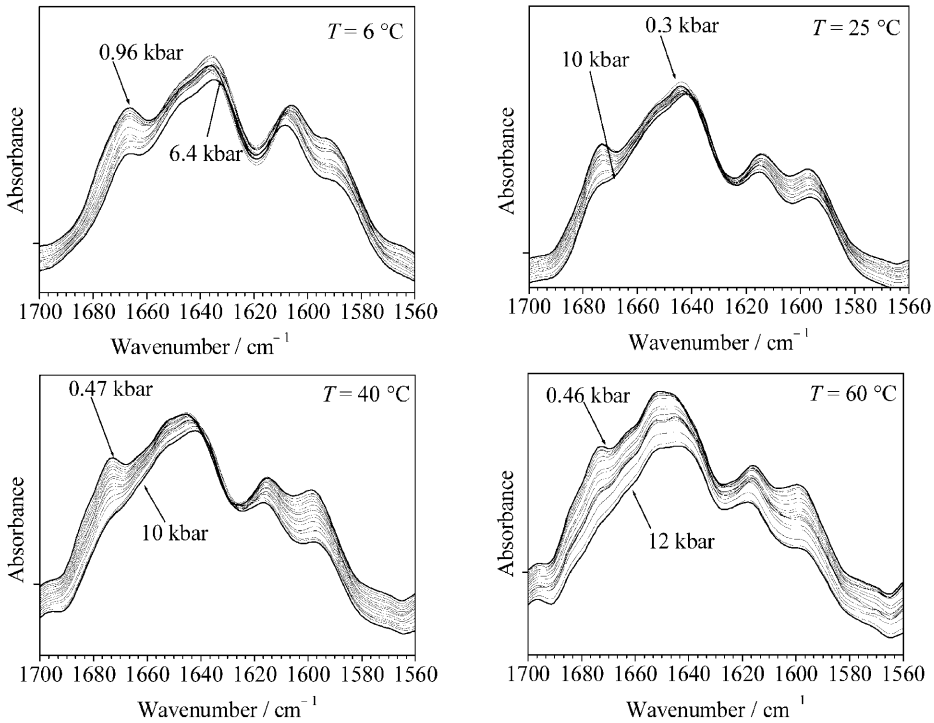

FIGURE 7 Deconvoluted FT-IR absorption spectra of the GVG(VPGVG) peptide at 5% (w/w), pD 7.0, as a function of pressure at four selected temperatures.

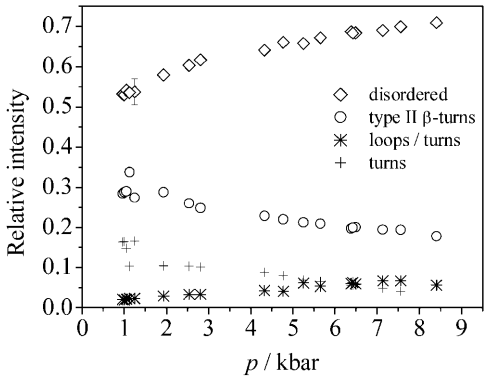

FIGURE 8 Relative intensities of secondary structure elements of the GVG(VPGVG) peptide as a function of pressure at 6°C and pD 7.0.

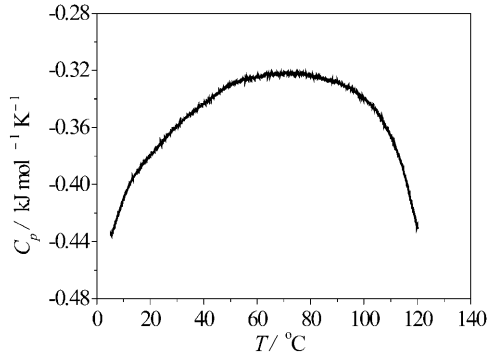

FIGURE 10 Heat capacity C_p of the GVG(VPGVG) peptide (measured with respect to the pure buffer solution) as a function of temperature at pD 7.0.

in an intermediate regime which corresponds to the more compact, folded loop state. In general, the folded state is characterized by lower α-values due to the lower surface-accessible surface area (Lin et al., 2002; Ravindra and Winter, 2003a,b). The increase in α at high temperature can be rationalized qualitatively in terms of a more pronounced hydration when the peptide starts to unfold again which leads to an increase of the SASA. Similarly, the apparent heat capacity of the peptide (measured relative to the pure buffer solution) is $C_p \approx -0.43$ kJ mol^{-1} K^{-1} at 2°C, increases initially and reaches a maximum of -0.33 kJ mol^{-1} K^{-1} at ~70°C, until it comes back at 120°C to its initial low-temperature values (Fig. 10). Thus, both thermodynamic quantities lead to the interpretation that at unusually high temperatures ($T \approx 120$°C), the octapeptide has changed its structure back to a state that is similar to the low-temperature one, whereas the intervening state is markedly different and more ordered. This behavior is in accord with the observation of a profound change in the dynamics of the peptide-water interface in the companion theoretical study (Rousseau et al., 2004).

SUMMARY

In this study, we investigated the temperature- and pressure-dependent structure and phase behavior of a solvated oligopeptide, GVG(VPGVG), which serves as a minimalistic elastin-like model system, over a large region of the phase field, ranging from 2 to 120°C and from ambient pressure up to ~10 kbar, applying both spectroscopic (CD, FT-IR) and thermodynamic (DSC, PPC) measurements. We find that this octapeptide behaves as a two-state system which undergoes the well-known inverse-temperature folding transition occurring over a broad temperature range around $T \approx 36$°C, and, in addition, a reentrant unfolding close to the boiling point of water ($T > 90$°C). Moreover, the pressure-dependence of the folding/unfolding transition was studied to yield a more complete picture of the p,T-stability diagram of the system. The data reveal, in accord with what would be expected from the general phase diagrams of monomeric proteins (Heremans and Smeller, 1998; Winter, 2002; Winter and Jonas, 1999; Balny et al., 2002; Ravindra and Winter, 2003a), that the folded state is destabilized upon application of high pressures. As a result, the population of disordered structures increases with increasing pressure. The underlying driving force is probably the decrease in ΔV as a result of the release of void volume in the folded state of the oligopeptide. Hence, these data suggest, rather unexpectedly, that elastins behave like other, ordinary proteins, with the crucial difference that the stability window of their folded (ordered) state approaches the boiling point of its solvent, water. This behavior is a consequence of the essentially hydrophobic nature of its amino acid residues, which, as a consequence, places the hydrophobic hydration contribution to the protein's stability among the prominent contributions. The thermodynamic data obtained suggest that the folding is a consequence of hydrophobic interactions being largely driven by the increase in entropy of water. In fact, the two-state folding/unfolding scenario, as inferred from the experiment is confirmed by a free energy order parameter analysis of MD data, and may also be tracked back to qualitative changes in the hydrogen-bond dynamics at the peptide/water interface (Rousseau et al., 2004). The MD simulations indicate large-amplitude opening and closing motions of the peptide that clearly have a stabilizing entropic

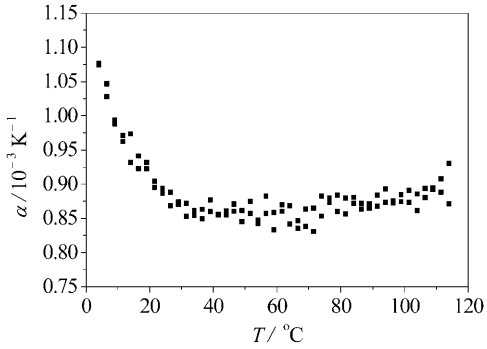

FIGURE 9 Apparent thermal expansion coefficient α of the GVG (VPGVG) peptide as a function of temperature at pD 7.0.

contribution to the observed folding behavior in the intermediate temperature range. This would be in accord with the maximum in C_p-value observed experimentally in this temperature regime, recalling that C_p is proportional to the entropy fluctuations $\langle(\delta S)^2\rangle$ of the system. Besides changes in conformational states, the shape of the C_p-T curve might also reflect changes in hydration of the amino acids as a function of temperature. Ultimately, at rather high temperatures, $T > 80°C$, the large librational amplitude motions of the peptide backbone can provide sufficient thermal excitation to break the peptide-peptide hydrogen bonds that ultimately leads to unfolding. This is probably best reflected in the subsequent decrease of C_p and the increase in the apparent coefficient of thermal expansion as a result of the increase of the SASA upon this second, unfolding transition.

Our work has greatly benefited from insightful and enjoyable discussions with Dominik Marx, Roger Rousseau, D. Paschek, and Alfons Geiger.

Financial support from the Deutsche Forschungsgemeinschaft (FOR 436) and the Fonds der Chemischen Industrie is gratefully acknowledged.

REFERENCES

Balny, C., P. Masson, and K. Heremans. 2002. High pressure effects on biological macromolecules: from structural changes to alteration of cellular processes. *Biochim. Biophys. Acta.* 1595:3–10.

Blokzijl, W., and J. B. F. N. Engberts. 1993. Hydrophobic effects: opinions and facts. *Angew. Chem. Int. Ed. (Engl.).* 32:1545–1579.

Byler, D. M., and H. Susi. 1986. Examination of the secondary structure of proteins by deconvoluted FTIR spectra. *Biochemistry.* 25:469–487.

Debelle, L., A. J. P. Alix, S. M. Wei, M. P. Jacob, J. P. Huvenne, M. Berjot, and P. Legrand. 1998. The secondary structure and architecture of human elastin. *J. Biochem.* 258:533–539.

Debelle, L., and A. J. P. Alix. 1999. The structures of elastins and their function. *Biochimie.* 81:981–994.

Debelle, L., and A. M. Tamburro. 1999. Elastin: molecular description and function. *Int. J. Biochem. Cell Biol.* 31:261–272.

Dzwolak, W., M. Kato, and Y. Taniguchi. 2002. Fourier transform infrared spectroscopy in high-pressure studies on proteins. *Biochim. Biophys. Acta.* 1596:131–144.

Herberhold, H., S. Marchal, R. Lange, C. H. Scheyhing, R. F. Vogel, and R. Winter. 2003. Characterization of the pressure-induced intermediate and unfolded state of red-shifted green fluorescent protein—a static and kinetic FTIR, UV/VIS and fluorescence spectroscopy study. *J. Mol. Biol.* 330:1153–1164.

Heremans, K., and L. Smeller. 1998. Protein structure and dynamics at high pressure. *Biochim. Biophys. Acta.* 1386:353–370.

Klink, B. U., R. Winter, M. Engelhard, and I. Chizhov. 2003. Pressure dependence of the photocycle kinetics of bacteriorhodopsin. *Biophys. J.* 83:3490–3498.

Li, B., D. O. V. Alonso, and V. Daggett. 2001. The molecular basis for the inverse temperature transition of elastin. *J. Mol. Biol.* 305:581–592.

Li, B., D. O. V. Alonso, B. J. Bennion, and V. Daggett. 2001. Hydrophobic hydration is an important source of elasticity in elastin-based biopolymers. *J. Am. Chem. Soc.* 123:11991–11998.

Lin, L. N., J. F. Brandts, J. M. Brandts, and V. Plotnikov. 2002. Determination of the volumetric properties of proteins and other solutes using pressure perturbation calorimetry. *Anal. Biochem.* 302:144–160.

Panick, G., R. Malessa, R. Winter, G. Rapp, K. J. Frye, and C. Royer. 1998. Structural characterization of the pressure-denatured state and folding/refolding kinetics of staphylococcal nuclease by synchrotron small-angle x-ray scattering and Fourier-transform infrared spectroscopy. *J. Mol. Biol.* 275:389–402.

Perczel, A., K. Park, and G. D. Fasman. 1992. Analysis of the circular dichroism spectrum of proteins using the convex constraint algorithm: a practical guide. *Anal. Biochem.* 203:83–93.

Perczel, A., M. Hollosi, G. Tusnady, and G. D. Fasman. 1991. Convex constraint analysis: a natural deconvolution of circular dichroism curves of proteins. *Protein Eng.* 4:669–679.

Pestrelski, S. J., D. M. Byler, and M. P. Thompson. 1991. Effect of metal ion binding on the secondary structure of bovine α-lactalbumin as examined by infrared spectroscopy. *Biochemistry.* 30:8797–8804.

Provencher, S. W., and J. Glöckner. 1981. Estimation of globular protein secondary structure from circular dichroism. *Biochemistry.* 20:33–37.

Ravindra, R., and R. Winter. 2003s. On the temperature-pressure free-energy landscape of proteins. *Chem. Phys. Chem.* 4:359–365.

Ravindra, R., and R. Winter. 2003b. Pressure perturbation calorimetric studies of the solvation properties and the thermal unfolding of proteins in solution. *Z. Phys. Chem.* 217:1221–1243.

Reiersen, H., A. R. Clarke, and A. R. Rees. 1998. Short elastin-like peptides exhibit the same temperature-induced structural transitions as elastin polymers: implications for protein engineering. *J. Mol. Biol.* 283:255–264.

Reis, O., R. Winter, and T. W. Zerda. 1996. The effect of high external pressure on DPPC-cholesterol multilamellar vesicles—a pressure-tuning Fourier-transform infrared spectroscopy study. *Biochim. Biophys. Acta.* 1279:5–16.

Rousseau, R., E. Schreiner, and A. Kohlmeyer. and Marx. 2004. Temperature-dependent conformational transitions and hydrogen-bond dynamics of the elastin-like octapeptide GVG(VPGVG): a molecular-dynamics study. *Biophys. J.* 86:1393–1407.

Siminovitch, D. J., P. T. T. Wong, and H. H. Mantsch. 1987. Effect of *cis* and *trans* unsaturation on the structure of phospholipid bilayers: a high-pressure infrared spectroscopic study. *Biochemistry.* 26:3277–3287.

Tamm, L., and A. Tatulian. 1997. Infrared spectroscopy of proteins and peptides in lipid bilayers. *Quart. Rev. Biophys.* 30:365–429.

Tarek, M., and D. J. Tobias. 1999. Environmental dependence of the dynamics of protein hydration water. *J. Am. Chem. Soc.* 121:9740–9741.

Tarek, M., and D. J. Tobias. 2002a. Role of protein-water hydrogen bond dynamics in the protein dynamical transition. *Phys. Rev. Lett.* 88:138101.

Tarek, M., and D. J. Tobias. 2002b. Single-particle and collective dynamics of protein hydration water: a molecular dynamics study. *Phys. Rev. Lett.* 89:275501.

Urry, D. W. 1993. Molecular machines: how motion and other functions of living organisms can result from reversible chemical changes. *Angew. Chem. Int. Ed.* 32:819–941.

Urry, D. W., R. G. Shaw, and K. U. Prasad. 1985. Polypentapeptide of elastin: temperature dependence of ellipticity and correlation with elastomeric force. *Biochem. Biophys. Res. Commun.* 130:50–57.

Urry, D. W., T. Hugel, M. Seit, H. E. Gaub, L. Sheiba, J. Dea, J. Xu, and T. Parker. 2002. Elastin: a representative ideal protein elastomer. *Phil. Trans. R. Soc. Lond. B.* 357:169–184.

Urry, D. W. 1997. Physical chemistry of biological free energy transduction as demonstrated by elastic protein-based polymers. *J. Phys. Chem. B.* 101:11007–11028.

Winter, R. 2002. Synchrotron x-ray and neutron small-angle scattering of lyotropic lipid mesophases, model biomembranes and proteins in solution at high pressure. *Biochim. Biophys. Acta.* 1595:160–184.

Winter, R., and J. Jonas, editors. 1999. High Pressure Molecular Science. NATO ASI E 358, Kluwer Academic Publishers, Dordrecht, The Netherlands.